RESPONSE OF A PILE SUPPORTED LNG STORAGE TANK DURING STRONG EARTHQUAKE

Daihachi OKAI[1], Takeyoshi NISIZAKI[2], Yasunari YANOU[3], Yozo GOTO[4] And Takashi MATSUDA[5]

SUMMARY

Strong earthquake response due to the 1995 Kobe Earthquake was recorded with 67 components including accelerations, strains, earth pressures and displacements on and around a large scale LNG storage tank located at 26km from the fault line. The tank stored LNG up to 70% of its capacity at the event. Maximum acceleration on the ground was 246gal, and maximum strain of the pile reached 333μ. This set of digital records can well describe the response of the tank and is invaluable to study the seismic safety of this kind of tank. The authors analyzed this data set and made clear followings: The acceleration and strain time series recorded on the tank and on its pile foundation reach their maximums during the principal part of SH wave incidence. Lowering of predominant frequency of the ground due to nonlinear response of subsurface soil can be seen during this principal part. Pile group effect appears so that the strains of the pile in the outer zone of the foundation are larger than those in the inside. Sloshing response of the contained LNG, 8.6 seconds in period, is detected by the strain sensors on the piles. Rocking response of the tank predominates than sway. Response amplification factors of the tank structure and the base slab on the basis of the subsurface ground are smaller than those applied to the design. Amplification on the incident wave by the subsurface ground is also smaller than that specified by the current design code. The response of the subsurface ground somewhat amplifies incident wave and is most influential to the seismic response of the tank and the piles. On the other hand, it damps the high frequency component of the wave that would excite the response of the tank.

INTRODUCTION

LNG, Liquid Natural Gas, is one of the important energy sources in Japan. More than 140 LNG storage tanks, total 10 mega-kiloliter capacity, are in operation. 65% of them are on-ground type, that are supported by pile group foundation. They have been designed in accordance with the design manual published by the Japan Gas Association [JGA, 1981] to have sufficient safety.

The authors started densely instrumented earthquake observation on one of the on-ground LNG storage tanks in 1983 [Kitamura et al, 1988]. The purpose of the observation is to improve more efficient seismic design method and to examine how much margin of seismic safety exists in the actual tank. The instrumented tank is situated on a reclaimed ground on the shore of Osaka bay, about 10 km south of Osaka City.

[1] *Osaka Gas Co. Ltd. Engineering Department, Osaka, Japan Fax:: 81-6-6231-1062*
[2] *Osaka Gas Co. Ltd. Engineering Department, Osaka, Japan Fax:: 81-6-6231-1062*
[3] *Osaka Gas Co. Ltd. Engineering Department, Osaka, Japan Fax:: 81-6-6231-1062*
[4] *Technical Research Institute of Obaysahi Corporation, Tokyo, Japan E-mail: KGE00351@nifty.ne.jp*
[5] *Technical Research Institute of Obaysahi Corporation, Tokyo, Japan E-mail: KGE00351@nifty.ne.jp*

Strong ground motion due to the 1995 Kobe earthquake hit this tank. The shortest length to the fault line is 26km. The observation system successfully recorded time series of 67 components that describe strong responses of the tank and the surrounding ground clearly.

Figure 1 shows the location of the tank and the fault line. Figure 2 and 3 are profiles of the tank and the surface soil. The inner tank is 57.6m in diameter and 28.8m in side wall height, made from 9% Ni steel of 8 to 27mm thickness, and contains at most 75,000 kiloliter of LNG, with a weight of 3.63MN. The outer tank holds heat insulator and does not contact to the inner. Both are placed on the double deck reinforced concrete slab, that is supported by 546 steel pipe piles, each of which is 609mm in diameter and 30m in length. The soft soil of 13m depth, that is based on deep alluvial and diluvial deposit. A reflection logging for deep layer has revealed that base rock appears at GL -1,340m and is horizontally stratified. Ring zone of the surface layer just around the pile foundation is improved by compaction method.

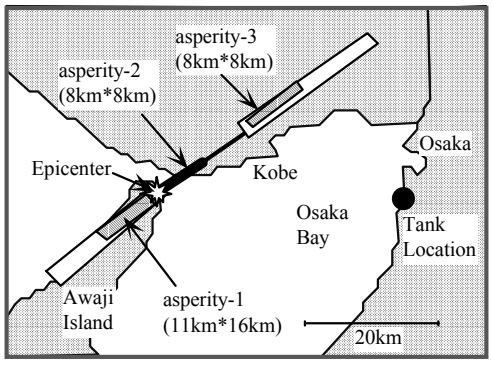

Figure 1 Location of Tank and Fault Line

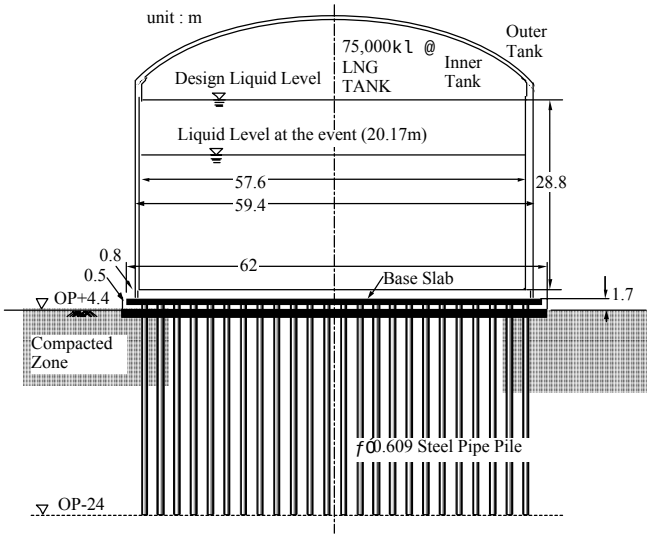

Figure 2 Profile of Tank

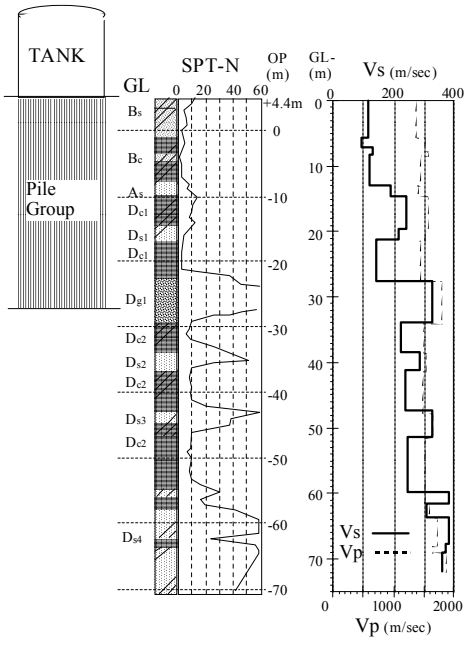

Figure 3 Soil Profile

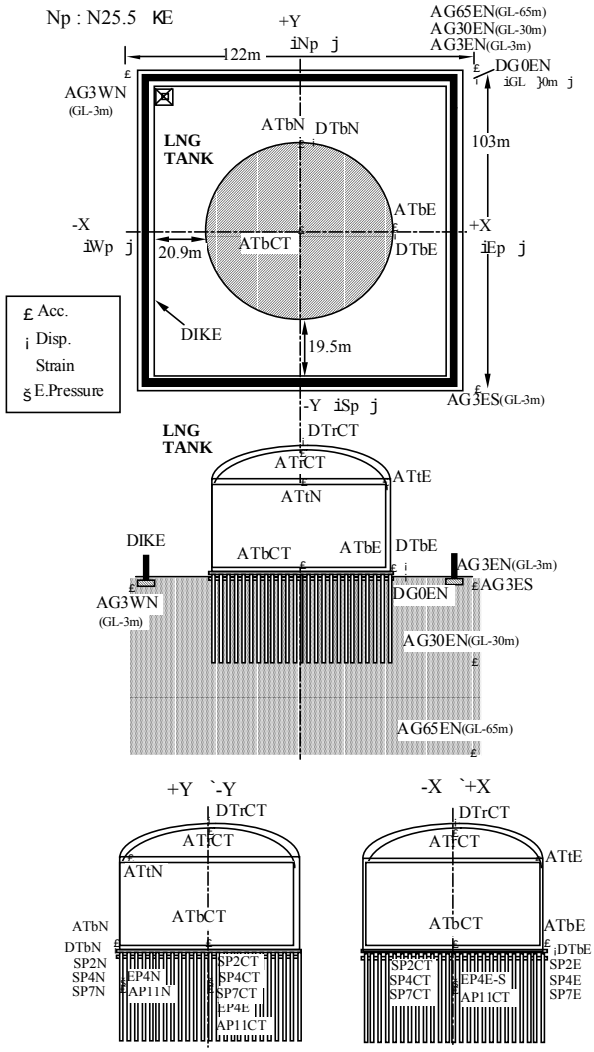

Figure 4 Instrumentation Arrangement

Figure 4 shows instrumentation arrangement. 19 accelerometers, most of them having three components, are distributed on the inner tank, on the base slab, on the piles, and in the surrounding ground. The accelerometers in the ground constitute a three dimensional array. 18 high sensitive strain gages as well as 4 displacement servo type earth-pressure cells are placed on the piles. 4 long period type displacement meters are located on the top of outer tank, on the base slab and on the ground.

Analog-digital converters with 16 bit resolution are used. All of the 67 channels are equipped with sample holders to erase time delay among channels springing from the digitization process. Record medium is magnetic tape, that could record the time series from 3 second before P-wave incidence on the support of buffer memories.

FEATURES OF INPUT GROUND MOTION

Figure 5 is a representative time history of acceleration. Incidence timings of P-wave, S-wave and surface wave estimated from the source mechanism model shown in Figure 1 [Irikura, et al. 1996] and the velocity structure model of Osaka basin [Kagawa, et al. 1993] are also plotted on Figure 5. It is remarked that all of the maximums of accelerations as well as strains occur within 10 seconds after S-wave incidence.

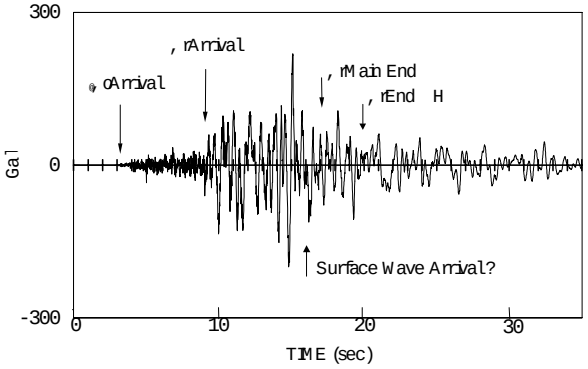

Figure 5 Incidences of P, S, Surface Waves

Figure 6 shows acceleration time histories obtained from a tripartite horizontal array around the tank, longest side of the triangle is 160m. Good coherence among the horizontal acceleration time histories is observed during the 10 seconds after S-wave incidence. In this paper, time series of this 10 seconds are applied to the analyses except the cases specially noted.

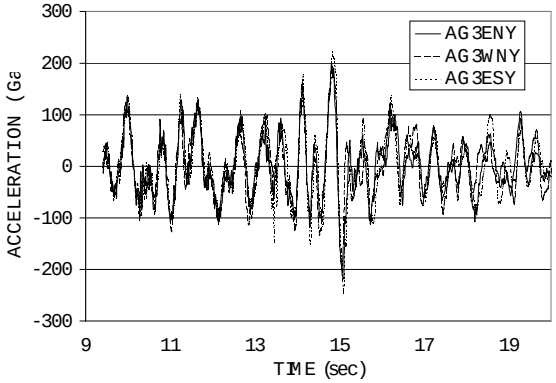

Figure 6 Coherence of Subsurface Acceleration

Figure 7 shows a typical velocity time history coming from integration of acceleration. High level coda wave exceeding 10 cm/second lasts for 2 minutes. It is one of the distinctive features of earthquakes in Osaka basin.

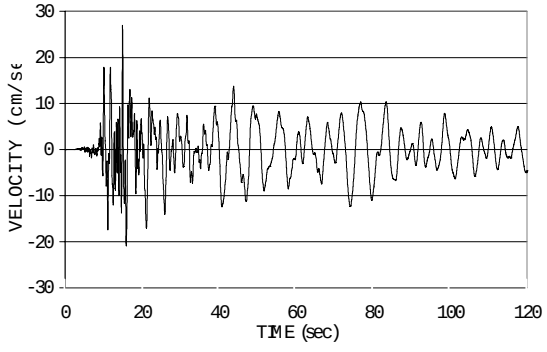

Figure 7 Velocity Time History

RESPONSE OF SUBSURFACE GROUND

Transfer function of horizontal motion, GL-3m/GL-65m, is shown in Figure 8 with a transfer function analyzed on a small after shock. All transfer functions presented in this paper are quotients of the absolutes of Fourier spectra smoothed by Parzen's spectral window of 0.2Hz band width. Amplifications up to the second mode predominate. Period elongation and amplification decreasing in the main event clearly appear on the first and second mode. The third mode that may be sensitive to the non-linear response of the upper subsurface ground disappear.

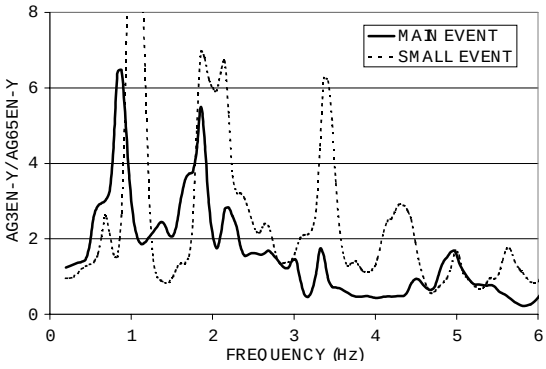

Figure 8 Transfer Function GL-3m/GL-65m

Figure 9 is non-stationary transfer function of the subsurface, GL-3m/GL-30m, that is quotient of non-stationary response power spectra proposed by Sugito, et al.[1984]. The predominant frequency sifts from 1.3Hz to 1.1Hz during the strong part of the ground motion and then goes back. Figure 10 shows long period variations of lateral earth-pressures recorded by the 4 earth-pressure cells attached on the piles at GL-3.7m in elevation. As the cells are under the water level in the ground, these variations may be outcome of the pore-water pressure rise, that is equivalent to about 20cm in water head.

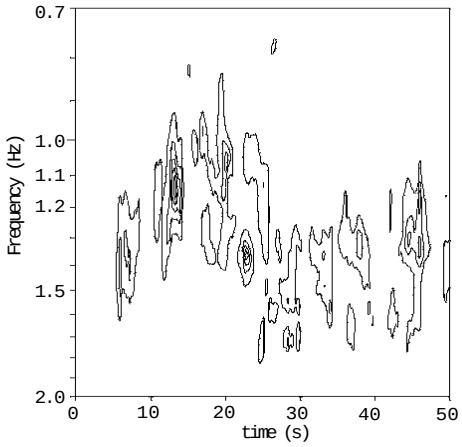

Figure 9 Non-stationary Transfer Function of Subsurface

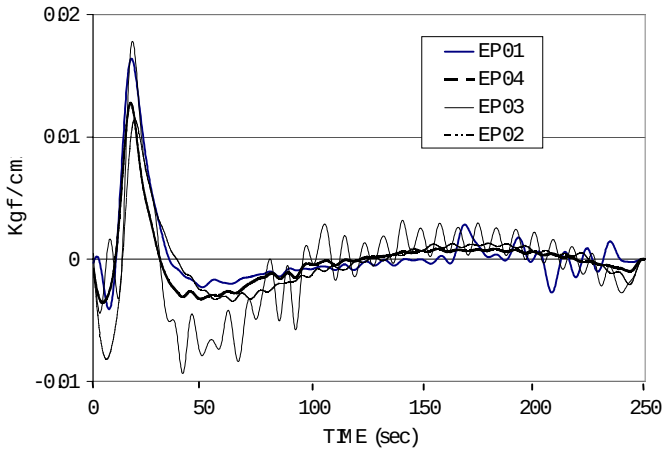

Figure 10 Long Period Variation of Earth Pressure (Filtered more than 5 sec)

RESPONSE OF TANK

Figure 11 is vertical distributions of maximum accelerations recorded on the tank and in the surrounding ground. The current design horizontal acceleration is also plotted. Although the observed acceleration on the top of the tank is larger than the twice of that of the pile tip level, the amplification from the bottom to the top is less than that of the specified in the design manual. The intensity of acceleration on the base slab becomes 80% of that of the ground surface due to the loss of effective input.

Figure 12 is transfer function of horizontal acceleration between the base slab and the ground at GL-3m. Sway response mode of the tank interacting with the ground as a rigid body predominates at 0.98Hz. The effective input drops in the frequency range between 1.5Hz and 3.5Hz. Figure 13 is transfer function of rocking

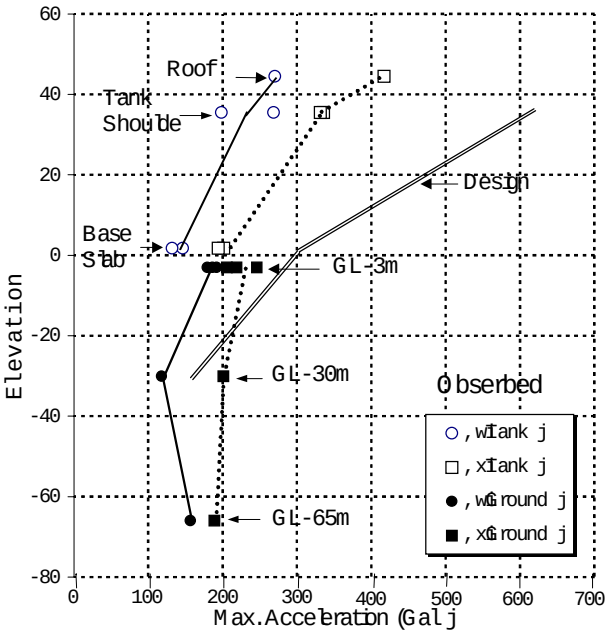

Figure 11 Max. Horizontal Acceleration

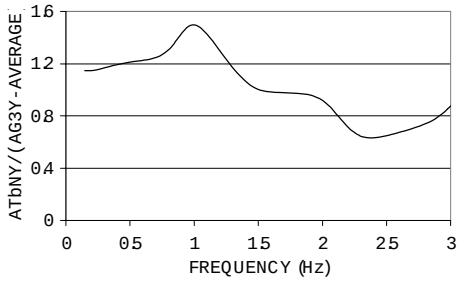

Figure 12 Sway Response of Tank Base

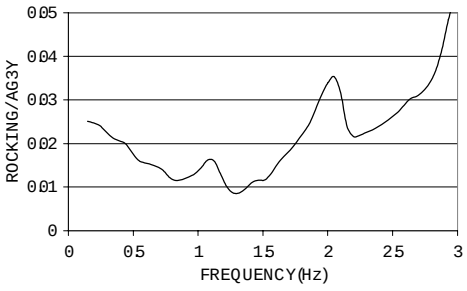

Figure 13 Rocking Response of Tank

acceleration of the tank, that is the difference between the horizontal acceleration of the tank shoulder and that of the base slab divided by the horizontal acceleration of the base slab. Rocking response mode of the tank predominates at 2.1Hz. Figure 14 is transfer function between the superstructure horizontal reaction and the base slab horizontal acceleration. The reaction is extracted from the strains of the piles, that are described later in this paper. When the amplitude of the base slab keeps constant, predominant peak of the reaction indicates a resonance of the superstructure. Then, the resonant frequency of the sway vibration of the tank superstructure is supposed to be 3.3Hz.

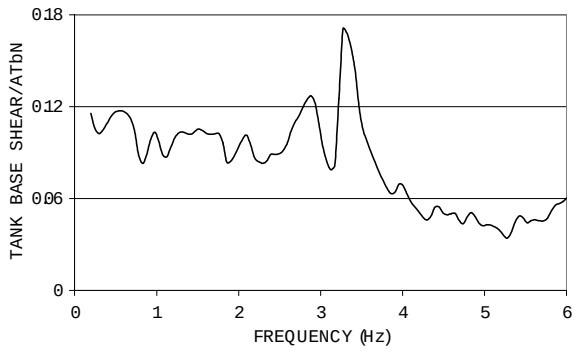

Figure 14 Response of Tank Superstructure

SLOSHING OF LNG

It is necessary to use sensors that cover such long period range as 10 second to analyze the sloshing response of the stored LNG. The authors used strains recorded on the piles and displacement recorded by the long period displacement meters. Figure 15 is Fourier spectrum of rocking moment of the pile group converted from the axial strains of piles (Detail is in the next chapter.). Time series of 250 seconds is analyzed applying 0.02 Hz as the band width for Parzen's spectral window. First predominant peak appears at 0.117Hz, that is the fundamental frequency of sloshing. Figure 16 and 17 show time histories of the rocking moment acting on the pile foundation and the displacement of the base slab, both of them are filtered by Chebyshev-I band pass filter. The pass range is from 0.6 to 1.7 times of the fundamental frequency. The component of the slab displacement having about 10 seconds in period reaches its maximum at 70 seconds after the S-wave incidence, and then the first mode of sloshing grows up. Once grown up, it is not easily damped even after the ground motion decreases. Rocking moment in the fundamental frequency range is about 7,000tonf*m,.

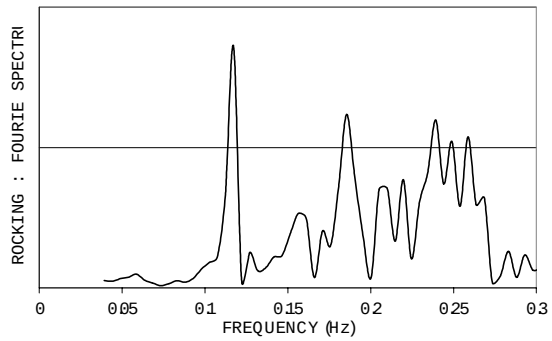

Figure 15 Rocking Moment of Pile Foundation

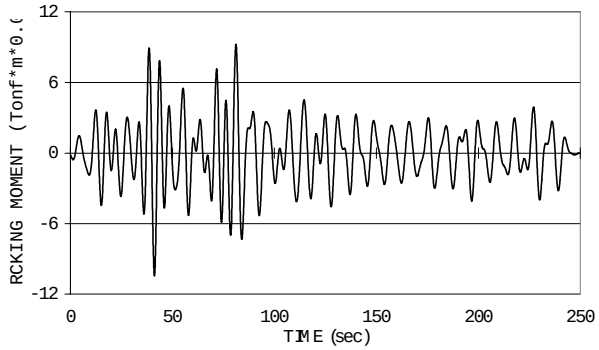

Figure 16 Rocking Moment of Pile Foundation

RESPONSE OF PILE GROUP

18 strain meters are located at three elevations of three piles, two of them located at the outer zone of the foundation (N_p-Edge and E_p-Edge) and one is in the central. The three elevations are GL-1.67m, -4.24m and -7.46m. A couple of strain meters is placed at each elevation so as to detect axial strain and bending strain in N_P-S_P direction. Table-1 is a list of the maximums of moment and axial force converted from the strains. Shear force and subgrade reaction that are extracted through differentiation of the moment are also listed. All of the maximums occurred around 5.6 seconds after the S-wave incidence. As the acceleration of ground in N_P-S_P direction is larger than that of E_P- W_P direction, axial force at N_P edge of pile group is 1.6 times larger than

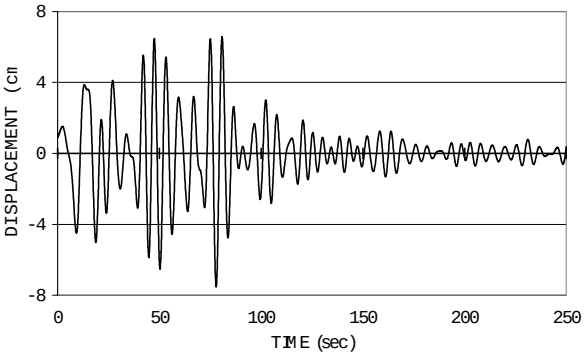

Figure 17 Sway Displacement of Slab

Table –1 Maximum Response of Piles

Location of Pile	N_p-Edge	E_p-Edge	Center
Axial Force (tonf)	42.8	27.09	19.69
Moment (tonf*cm)	2709.0	3074.0	1860.0
Shear Force (tonf)	7.881	10.33	5.811
Subgrade Reaction (tonf/cm)	0.02072	0.02506	0.01171

that at the E_P edge. Concerning the moment, the shear force and the subgrade reaction, order of the magnitudes is depending on their location, namely, E_P edge > N_P edge > Center. This order is consistent with the pile group effect, that reduces the responses of piles in the center and is most ineffective to the E_P edge pile as far as E_P-S_P direction concerned. Figure 18 compares Fourier spectrums of horizontal acceleration time series observed on a pile located at the center of the pile group with that observed on a pile located at the N_P edge at the same elevation GL-11m. The central pile and the edge pile respond coherently in the lower frequency range less than 1.5Hz. The response of the central pile predominates in the middle frequency range, 1.5 - 3.2Hz, while the edge pile predominates in the higher frequency range. It is supposed that the pile group pushes and pulls the surrounding ground in the middle frequency rang and the surrounding ground pushes and pulls the pile group in the higher frequency range at the GL-11m elevation.

Figure 19 is a hysteresis loop between earth pressure and relative displacement during 4 seconds just after the S-wave incidence. The earth pressure time series is from the earth pressure cell located on the outside of N_P edge pile at GL-3.7m elevation. The consistency of this observed pressure is assured by the comparison with shear force distribution extracted from the observed strains of the pile. The relative displacement time series is from the deference between the double integrals of accelerations at the GL-3m and the base slab. And these two time series are filtered with pass range from 0.8Hz to 3.0Hz. The coefficient of subgrade reaction observed in Figure

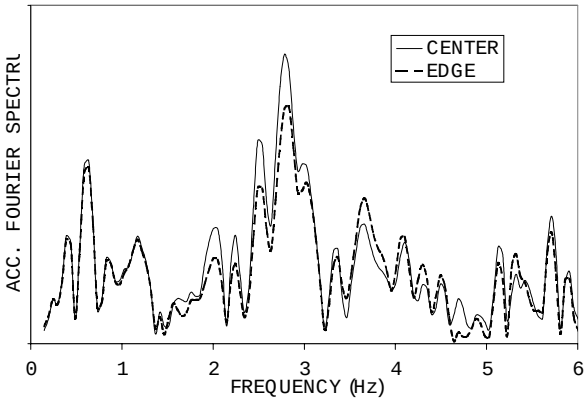

Figure 18 Responses of Center and Edge Pile

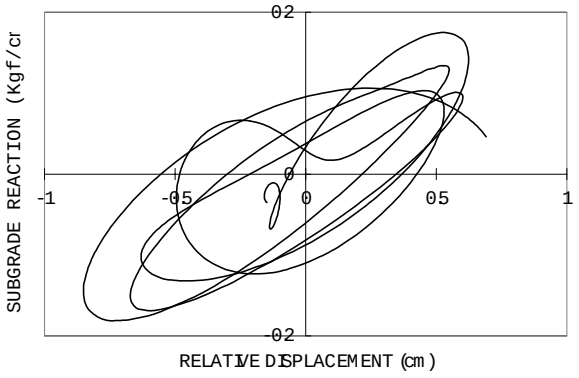

Figure 19 Hysteresis of Subgrade Reaction

19 is such small value as 0.2kg/cm^3, that is supposed to be the outcome of the pile group effect.
Superstructure reaction shall be equal to total shear force on the pile heads, that is approximately to be the product of total number of piles, 546, by the average of shear force detected at the three instrumented piles. Figure 20 compares time history of the total pile head shear with that of the superstructure, that is product of the base slab acceleration by the sum of mass of base slab, mass of tank structure and effective mass of fluid. As the total shear is somewhat shorts, subgrade reaction acting on the base slab is supposed to share the superstructure reaction. Adding further, subsurface ground around the base slab is paved by heat insulating concrete based on leveling concrete slab. Total thickness of these two pavements is 20cm, and new cracks were not found in the pavement just around the base slab after the earthquake.

Figure 21 is transfer function between time series of total rotational moment and total shear force on the pile head. The total rotational moment is derived from the distribution of the axial forces of piles assuming plane distribution, inclination of which is defined by the difference of the axial forces between the edge pile and the center pile. The vertical axis of Figure 21 must indicate the height of inertia center of the superstructure in the frequency range less than the first resonance of the superstructure if the horizontal reaction does not spill away from the base slab. The extracted height is somewhat larger than that of the estimated, and this discrepancy indicates that the subgrade reaction acting on the base slab is not negligible.

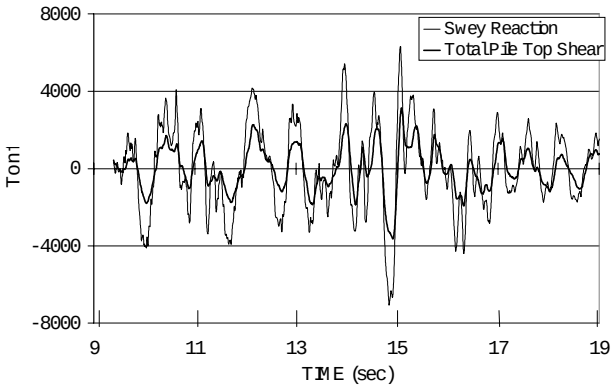

Figure 20 Superstructure Reaction & Pile Top Shear

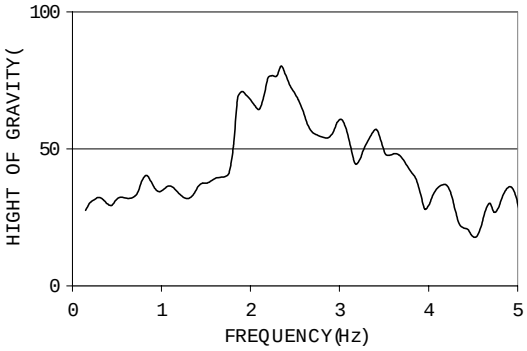

Figure 21 Total Moment/Total Shear

DESTRUCTIVE POTENTIAL OF EACH MODE

It is important for engineering practice to know the destructive potential of earthquake response of each mode. Although the excitation of each mode depends on the character of earthquake, the authors assume this earthquake to be a typical case and analyze the ratio of contribution of each mode to the velocity time series on the top of the tank and to the strain time series on the pile. Namely, these observed time series are filtered with bandpass filter having the central frequency as same as the predominant frequency of each mode and the band width 0.9 – 1.1 times of the central frequency. Velocity and strain are concerned here as they are consistent with destructive potential. Maximums of the filtered time series occur within 13 second after the S-wave incidence except the sloshing, the potential of which is smaller by one digit than the others. Figure 22 and 23 show the maximums comparatively. Consequences of the predominant modes of the subsurface ground are larger than those of the predominant modes of structure such as rocking and sway. It can be said that the reclaimed soft ground takes two roles at the same time, as an amplifier of the ground motion and as an isolator for the structure response. The strain on the edge pile is more affected by the predominant modes of the ground than that of the center pile. It is because not only the effect of pile group but also the overturning moment caused by the horizontal acceleration acting on the superstructure.

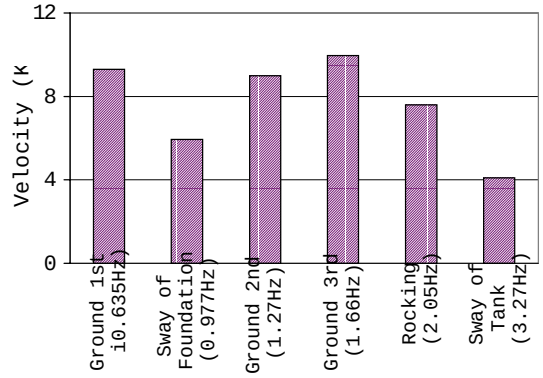

Figure 22 Maximum Velocity at Tank Top

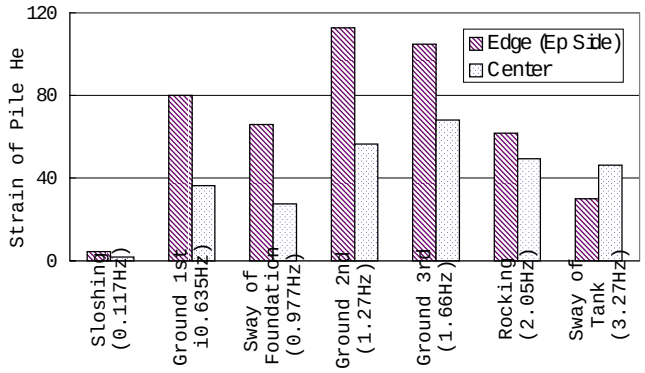

Figure 23 Maximum Strain at Pile Top

COMPARISON WITH CURRENT DESIGN FORMULAS

Table 2 compares the frequencies and the amplification factors of the predominant modes extracted from the observed time series with those estimated from current design formulas. The observed amplification factor is defined by the ratio of the maximum of band pass filtered time series of the representative point with that of the base point. The observed frequencies of tank sway response and roof sway response are somewhat smaller than those of the estimated, but the others are in good coincidence. All of the observed amplification factors are smaller than those of the estimated. As far as the amplification factors extracted in this study are referred to, the amplification factors evaluated from the current design formulas are in safety side. Table 3 shows the subgrade reaction factor. When the observed value 0.2kgf/cm^3 is compared to the current formula value for single pile, it is

too small. When the reduction by the pile group effect is assumed to follow the square root of N rule (N: Total number of piles), the current formula value becomes consistent with the observed. But, it should be noted that the observed factor is the outcome of the earth pressure cell located on the outside of the outer edge pile that does not represent the average. In any ways, the pile group effect shall be carefully considered in the seismic response analyses for this kind of multiple piles foundation.

Table-2 Comparison of Observed Frequency and Amplification with Those of Design

	Designed Frequency	Observed Frequency	Designed Amplification	Observed Amplification
Sway of Tank	4.12 Hz	3.27 Hz	2.07	2.0
Sway of Roof	6.69	5.80	1.66	1.3
Up-Down	4.17	4.35	4.17	2.8
Rocking	2.02	2.05		
Sloshing	0.117	0.117	9.4	5.0
Subsurface Ground			2.0	1.2

Table-3 Comparison of Subgrade Reaction

Observed Subgrade Reaction Factor	0.2Kgf/cm^3
Design Formula Value for Single Pile	4.1
Pile Group Effect Considered to Above	0.18

CONCLUSION

1. The strong earthquake response of an on ground LNG tank founded on hundreds of piles was successfully recorded by 67 channels earthquake observation system during the 1995 Kobe earthquake.
2. Accelerations and velocities on the tank and in the surrounding ground as well as strains of the piles reached their maximum during the principal part of SH-wave incidence, where as sloshing of the stored fluid predominated 70 seconds after the SH-wave incidence.
3. Although maximum horizontal acceleration at the top of the tank was a twice of the maximum acceleration at the GL-65m ground, the amplification taken into account in the seismic design is larger than the observed.
4. Lowering of predominant frequency of the ground due to the softening of subsurface soil occurred during the strong S-wave incidence.
5. Predominant modes such as rocking, sway and vertical response of the tank are clearly extracted from the recorded time series. As their frequencies are consistent with and their amplification factors are smaller than those evaluated from design formula, the current design is assured to have sufficient safety margin.
6. Strains of piles in the outer area of the pile group are larger than those in the central area because of the pile group effect. Subgrade reaction factor extracted from the recorded time series of earth pressure is considerably smaller than that of the current design for single pile. This discrepancy is also supposed to be the outcome of the pile group effect.
7. The reclaimed soft ground takes two roles at the same time, as an amplifier of ground motion and as an isolator for structure response.

ACKNOWLEDGEMENTS

The authors would like to express their deep appreciation to Professor Kenzo Toki of Kyoto University and Professor Hiroshi Akiyama of Nippon University for their kind advises on this study, and to Dr. Hachiro Kitamura and Mr. Koji Yanabu of Osaka Gas Co. Ltd., for their continuous effort and support to set and maintain this invaluable observation system.

REFERENCES

1. Committee on LNG Aboveground Storage, Japan Gas Association (1981):*Recommended Practice for LNG Aboveground Storage,* Special Publication of Japan Gas Association
2. Sugito, M.,Goto, H. and Akikawa, F. (1984):*Simplified Separation Technique of Body and Surface Wave in Strong Motion Accelerograms,* Proc. of JSCE Vol. 1, No.2, pp.185-190
3. Kitamura, H., Yanabu, K. and Goto, Y. (1988):*Studies on Earthquake Response of On-ground LNG Storage Tank Based on Observed Records*, Vol. , Proc. Ninth WCEE, pp703-708
4. Kagawa, T., Sawada, Y., Iwasaki, Y. and Nanjo, A. (1993):*On the Modelization of Deep Sedimentary Structure beneath the Osaka Plain*, Abstr., Seismol. Soc. Jpn.,2,pp.112-117 (in Japanese)
5. Irikura, K. and Kamae, K. (1996):Physically Based Source Models and Strong-Ground-Motion Prediction, Proc. Eleventh WCEE